



## Molecular docking analysis of 2,4,6-Octatrienoic acid with apoptotic protein targets: Insights into potential biological interactions

Shanmugam M Sivasankaran<sup>1</sup>, Raju Kowsalya<sup>1\*</sup>, Krishnan Baskaran<sup>3</sup>, A. Therasa Alphonsa<sup>2</sup>, Virumandi Sethupathi<sup>1</sup> and Chakravarthy Elanchezhian<sup>4</sup>

<sup>1</sup>Department of Biochemistry and Biotechnology, Annamalai University, Annamalainagar - 608002, Tamilnadu, India.

<sup>2</sup>Department of Chemistry, Annamalai University, Annamalainagar - 608002, Tamilnadu, India

<sup>3</sup>Department of Biochemistry, Madha Medical College and Research Institute, Chennai-600128, Tamilnadu, India.

<sup>4</sup>Department of Zoology, Annamalai University, Annamalainagar-608002, Tamilnadu, India.

### ARTICLE INFO

#### Article history:

Received 30 December 2024

Revised 07 February 2025

Accepted 16 February 2025

Published online 01 April 2025

**Copyright:** © 2025 Sivasankaran *et al.* This is an open-access article distributed under the terms of the [Creative Commons Attribution License](https://creativecommons.org/licenses/by/4.0/), which permits unrestricted use, distribution, and reproduction in any medium, provided the original author and source are credited.

### ABSTRACT

The discovery of novel compounds targeting apoptotic pathways presents significant potential for therapeutic advancements in cancer and other diseases marked by impaired apoptotic regulation. Dysregulation of apoptosis is a hallmark of various diseases, including cancer, neurodegenerative disorders, and autoimmune conditions. Therefore, identifying small molecules capable of modulating apoptotic pathways has gained considerable attention in drug discovery. In this study, the binding affinity and interaction dynamics of 2,4,6-Octatrienoic acid were evaluated through molecular docking with key apoptotic regulators, including pro-apoptotic, anti-apoptotic, and regulatory proteins. Docking simulations demonstrated strong binding affinities of 2,4,6-Octatrienoic acid to Caspase-7, BAX, Bcl-2-like protein 1, Bcl-2-like protein 2, Mcl-1, XIAP, and Apoptosis-inducing factor 1, with respective docking scores of -4.242, -3.427, -3.676, -2.917, -4.625, -3.007, and -3.593. These findings suggest its potential role in modulating apoptotic pathways. Interaction analyses revealed the presence of hydrogen bonding, hydrophobic interactions, and van der Waals forces, stabilizing these proteins in either their active or inhibited states. This suggests that 2,4,6-Octatrienoic acid may influence apoptosis by inducing programmed cell death in cancer cells or preventing excessive apoptosis in degenerative conditions. Overall, this study highlights 2,4,6-Octatrienoic acid as a promising candidate for apoptosis-targeted drug development. Future research should focus on detailed molecular dynamics simulations, structural modifications and preclinical evaluations to determine its efficacy in disease models. Further *in vitro* and *in vivo* studies are essential to validate these results and to explore the compound's therapeutic efficacy in greater depth.

**Keywords:** 2,4,6-Octatrienoic acid, Molecular docking, Apoptotic proteins.

### Introduction

Apoptosis or programmed cell death is a vital biological process essential for maintaining cellular homeostasis.<sup>1</sup> Its dysregulation is implicated in various pathological conditions, including cancer.<sup>2,3</sup> As a result, targeting apoptotic pathways has gained prominence as a promising strategy for therapeutic intervention. Molecular docking has emerged as a powerful tool in drug discovery, enabling precise predictions of interactions between small molecules and biological targets.<sup>4</sup> Despite significant advancements in this field, the quest for novel compounds with high specificity toward apoptotic markers remains critical. This study explores the therapeutic potential of 2,4,6-Octatrienoic acid through its interactions with key apoptotic markers. 2,4,6-Octatrienoic acid, also known as (2E,4E,6E)-Octa-2,4,6-trienoic acid, is a small polyunsaturated carboxylic acid with the molecular formula C<sub>8</sub>H<sub>10</sub>O<sub>2</sub> and a molecular weight of 138.16 g/mol. This compound features a unique structure consisting of an eight carbon chain with three conjugated double bonds, which contribute to its high

chemical reactivity. These conjugated bonds play a pivotal role in its behaviour during light-induced reactions, polymerization, photoisomerization, and peroxidation. Biologically, compounds like 2,4,6-Octatrienoic acid are often involved in signaling pathways, lipid metabolism, and responses to cellular stress. A notable natural source of this molecule is *Deschampsia antarctica* (Antarctic hair grass), highlighting its ecological and biochemical significance. *Deschampsia antarctica* is one of the only two vascular plants native to Antarctica, demonstrating extraordinary resilience in extreme environments characterized by subzero temperatures, intense UV radiation, and nutrient-deficient soils. Ecologically, it plays a fundamental role in stabilizing soil, sequestering carbon, and fostering microbial interactions essential for ecosystem sustainability. Biochemically, it has evolved sophisticated defense mechanisms, including the synthesis of antifreeze proteins (AFPs) to mitigate ice damage, antioxidants to neutralize oxidative stress, and UV-absorbing compounds to protect against radiation-induced damage. Furthermore, its unique biochemical profile presents promising opportunities for advancements in biotechnology, with potential applications in agriculture, medicine, and cosmetic industries.<sup>5-7</sup>

Traditional wet-lab methods in drug discovery, while comprehensive, are time-consuming and costly when screening large numbers of drug candidates. In contrast, *in silico* approaches, such as molecular docking, offer efficient and cost-effective alternatives for high-throughput screening and facilitate the prediction of precise binding affinities, providing critical insights into target specificity and compound efficiency, which are essential for advancing therapeutic research.<sup>8,9</sup>

\*Corresponding author. E mail: [kowsalyamouli@yahoo.com](mailto:kowsalyamouli@yahoo.com)

Tel: +91 8248507945

**Citation:** Sivasankaran SM, Kowsalya R, Baskaran K, Alphonsa AT, Sethupathi V and Elanchezhian C Trop J Nat Prod Res. 2025; 9(3): 1346 – 1357 <https://doi.org/10.26538/tjnpr/v9i3.60>

Official Journal of Natural Product Research Group, Faculty of Pharmacy, University of Benin, Benin City, Nigeria

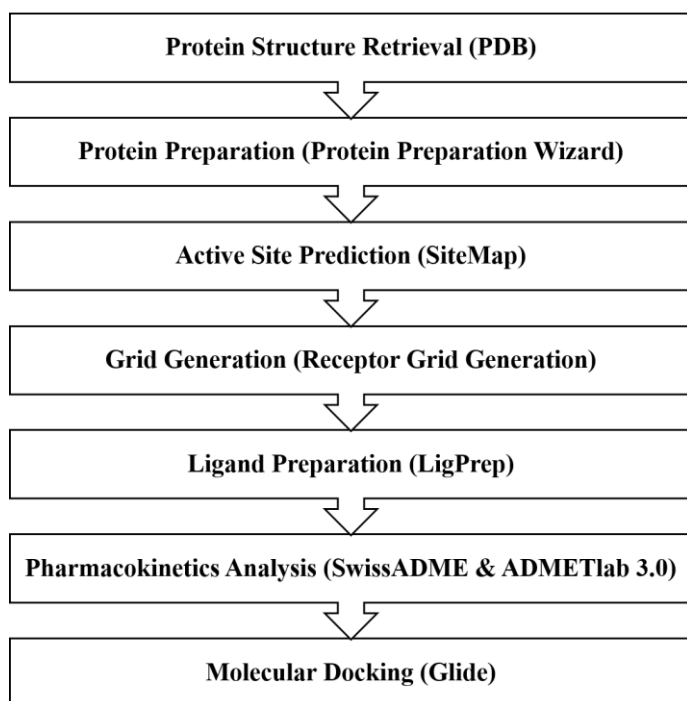
This study focused on docking 2,4,6-Octatrienoic acid against 20 apoptotic proteins to identify the most promising target.

## Materials and Methods

### Software, databases, and tools

Schrödinger, Inc. is a software company that provides various computational tools for drug discovery and material science. Here, the Maestro suite from the Schrodinger (2024-1) software was used to accomplish the entire task required for molecular docking analysis. Protein Data Bank (PDB) is a database utilised in this study to retrieve three-dimensional (3D) structures of the proteins.<sup>10</sup> The compound 2,4,6-Octatrienoic acid was downloaded as an SDF file from the PubChem chemical database. SwissADME and ADMET Lab 3.0 are two different tools that analyse the pharmacokinetic properties of the given ligand comprehensively. The molecular docking workflow was carried out following a systematic approach, including protein and ligand preparation, active site prediction, grid generation, docking, and pharmacokinetics analysis. The overall process is illustrated in figure 1.

**Figure 1:** Molecular Docking Workflow



### Protein retrieval and preparation

We identified the comprehensive list of 20 key proteins involved in both intrinsic and extrinsic pathways of apoptosis, and the 3D structures were retrieved from the PDB database. As the retrieved proteins are not readily available for molecular docking analysis, we should prepare the protein. This step was done by a protein preparation wizard from the Maestro suite. Missing residues and side chains were fixed, bond order was assigned, and the protonation state was adjusted, hydrogen bonding networks were optimised, and the water molecules beyond 5 Å from the active site were removed; most importantly, energy minimisation was done to relieve steric clashes.

### Active site prediction

Along with preparing the protein for the molecular docking analysis, it is important to identify the place where the ligand of interest will bind to our protein of interest. The active site and binding site information for all the proteins is limited, which forces us to find an alternative. Here, we used SiteMap from Maestro to predict the potential binding pockets based on the two important scoring functions. One is SiteScore, which will predict the binding pocket properties, and the DScore scoring function measures the druggability. The site with the highest

SiteScore and DScore was selected from the top possible predicted binding sites.

### Receptor grid generation

The grid box was generated around the predicted active site using the receptor grid generation from the Maestro suite. The grid box dimensions were set to 20 Å × 20 Å × 20 Å, centred on the centroid of the active site residues. The default van der Waals scaling (1.0) and partial charge cutoff (0.25) were applied. The generated grid file was saved and used for molecular docking analysis.

### Ligand preparation

The Ligprep tool from the Maestro suite was used in the preparation process, in which the possible tautomers and stereoisomers were generated. The OPLS4 force field was optimised for the ligand geometries, and the protonation state was assigned at physiological pH (7.0 ± 2.0) using Epik. The output file was saved in Maestro format for docking.

### Pharmacokinetic analysis

#### SwissADME

This tool is used to analyse the drug-likeness, physiochemical properties and pharmacokinetic profiles of the ligand. The prepared ligand were saved in SDF format and inputted to the SwissADME web server.<sup>11</sup> The parameters are left default; the predictions include molecular weight, lipophilicity, hydrogen bond donors and acceptors, topological polar surface area, and Lipinski's rule of five. Further, the results was analysed to assess drug-likeness, solubility, pharmacokinetic properties such as gastrointestinal absorption and blood-brain barrier permeability, and synthetic accessibility.

#### ADMETLab 3.0

This tool provides a comprehensive evaluation of ADMET (Absorption, Distribution, Metabolism, Excretion, and Toxicity) properties. The ligand structure was uploaded to the ADMETLab 3.0 web server in SMILES format.<sup>12</sup> The absorption properties, such as Caco-2 permeability and human intestinal absorption; the distribution properties, including plasma protein binding and volume of distribution; the metabolism profiles, such as cytochrome P450 inhibition; and the toxicity properties, such as Ames toxicity, hERG inhibition, and hepatotoxicity, were calculated. The favourable properties, such as high absorption and low toxicity, made the ligand more likely to be chosen for molecular docking analysis.

### Molecular Docking

Molecular docking aims to generate the possible and energetically favourable protein-ligand complex from the known protein structures and known ligands in a fraction of time. Here, the ligand-based screening was done by the Ligand docking module from the Maestro suite. The prepared protein (n=20) was screened against the prepared ligand; the parameters were set to extra precision (XP) for higher accuracy. The complex with favourable binding energy was further evaluated. The protein-ligand interaction was visualised by the Maestro visualisation tool, and the top-ranked poses were selected based on the scoring functions.

## Results and Discussion

Apoptosis, a natural biological process of programmed cell death, plays a crucial role in human development, fostering a healthy immune system by eliminating pre-cancerous and virus-infected cells, and maintaining cellular balance. Apoptosis can be triggered through extrinsic and intrinsic pathways that are regulated by two key groups of molecules, Bax and Bcl-2. When apoptotic signaling functions correctly, unwanted cells are efficiently removed from the body. However, in conditions like cancer, cells acquire the ability to evade apoptosis, leading to uncontrolled proliferation. By eliminating harmful cells, apoptosis not only prevents disease but also supports the immune system's overall health and balance. Bcl-2 has emerged as a pivotal target in cancer therapy due to its role in regulating apoptosis.<sup>13,14 15</sup> explored the development of novel drugs designed to target Bcl-2,

aiming to induce apoptosis in cancer cells and enhance the efficacy of treatments such as chemotherapy. <sup>16</sup> investigated the bioactive compounds derived from *Annona muricata* Linn as potential inhibitors of the anti-apoptotic proteins Bcl-2, Bcl-w, and Mcl-1 through molecular docking studies. <sup>17</sup> conducted a comprehensive investigation into the anticancer potential of trisindoline derivatives through molecular docking studies, specifically targeting key apoptotic regulators, p53 and caspase-9. <sup>18</sup> explored the anticancer potential of Cytotoxin 10 by assessing its effects on the expression of key apoptosis-related proteins, including Bax, Bcl-2, Caspase-7, and PARP, in treated cell lines. The present study explores the molecular docking analysis of 2,4,6-Octatrienoic acid with apoptotic protein targets. The molecular docking results are summarized in Tables 1-3. The molecular docking analysis revealed a strong binding affinity of 2,4,6-Octatrienoic acid with key apoptotic markers.

Table 1 presents the docking scores and structural characteristics of 12 key pro-apoptotic proteins, highlighting their potential interactions and functional significance in apoptosis. Apoptosis regulator BAX, with a resolution of 1.80 Å, forms a hetero 4-mer comprising 192 residues and exhibits a docking score of -3.427, indicating strong binding potential. The Bcl-2 homologous antagonist/killer, resolved at 1.48 Å as a homo 2-mer with 211 residues, shows a docking score of -1.070, suggesting moderate binding affinity. Similarly, the Bcl2-associated agonist of cell death, with a resolution of 2.36 Å and 168 residues, demonstrates a docking score of -2.556, reflecting favorable interaction potential. The

BH3-interacting domain death agonist, resolved at 1.41 Å as a hetero 2-mer with 195 residues, has a docking score of -1.494, while the Bcl-2-binding component 3, with a resolution of 1.33 Å as a hetero 2-mer containing 193 residues, shows a docking score of -2.300, indicating favorable binding interactions. The phorbol-12-myristate-13-acetate-induced protein 1, resolved at 2.24 Å with 54 residues, exhibits a docking score of -2.359, suggesting significant interaction potential. Apoptotic protease-activating factor 1, the largest structure in this analysis, forms a hetero 14-mer with 1248 residues and is resolved at 3.80 Å, though no docking score is available for this protein. Caspase-8, resolved at 1.20 Å as a hetero 6-mer with 479 residues, presents a docking score of -2.241, indicating strong binding potential, whereas caspase-9, with a resolution of 2.40 Å and 416 residues, exhibits a docking score of -2.013. Caspase-3, resolved at 1.40 Å as a hetero 8-mer with 277 residues, has a docking score of -1.354, suggesting moderate binding affinity. Caspase-6, with a resolution of 1.63 Å as a hetero 4-mer consisting of 293 residues, displays a docking score of -1.859. Finally, caspase-7, resolved at 1.65 Å with 303 residues, exhibits the most favorable docking score of -4.242, indicating the strongest interaction potential among the analyzed proteins. These docking scores highlight varying binding affinities, with proteins like Caspase-7 and BAX standing out for their strong interaction potential, making them attractive candidates for therapeutic targeting. Structural details further enrich the understanding of their functional roles in apoptotic pathways. The nearest high score binding images are described in figures 2 and 3 (3D and 2D images).

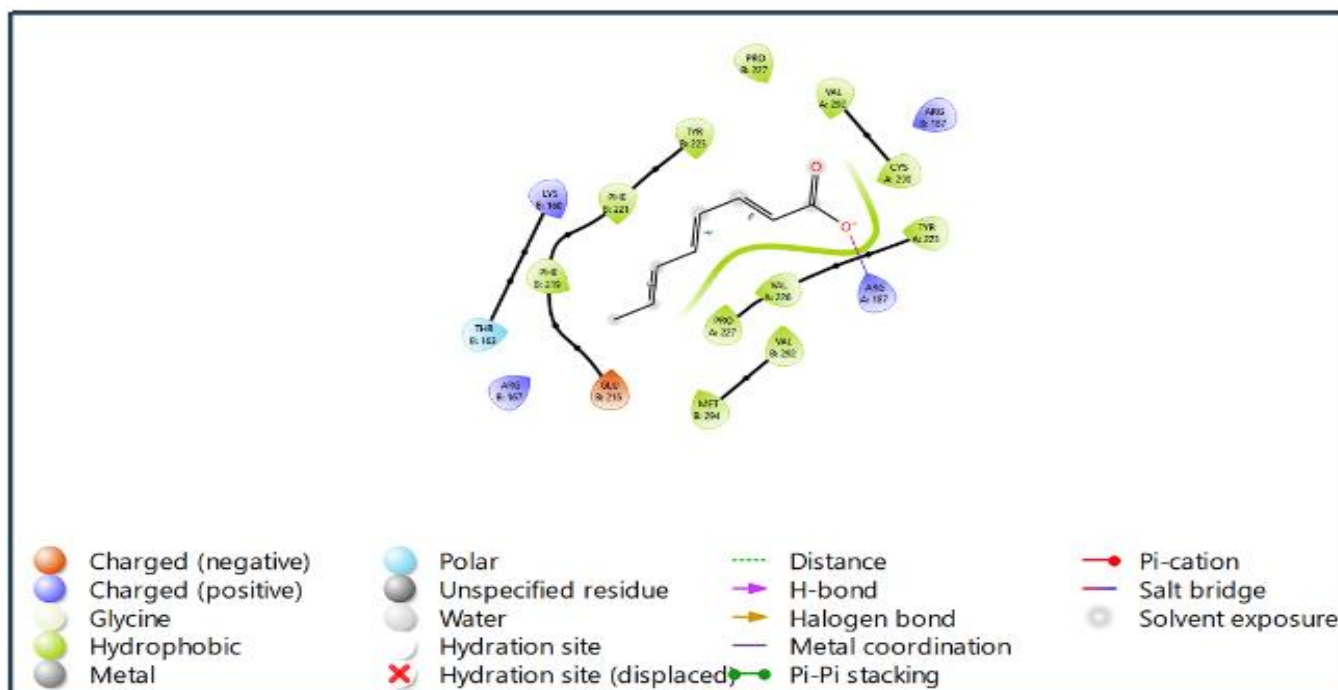
**Table 1:** The docking scores and structural details of 12 critical pro-apoptotic proteins

Uniprot ID	PDB ID	Protein Name	Resolution (Å)	Global Stoichiometry	Residues	Docking Score
Q07812	4ZIE	Apoptosis regulator BAX	1.80 Å	Hetero 4-mer	192	-3.427
Q16611	2IMS	Bcl-2 homologous antagonist/killer	1.48 Å	Homo 2-mer	211	-1.070
Q92934	7Q16	Bcl2-associated agonist of cell death	2.36 Å	Homo 2-mer	168	-2.556
P55957	7QTW	BH3-interacting domain death agonist	1.41 Å	Hetero 2-mer	195	-1.494
Q9BXH1	5UUL	Bcl-2-binding component 3	1.33 Å	Hetero 2-mer	193	-2.300
Q13794	3MQP	Phorbol-12-myristate-13-acetate-induced protein 1	2.24 Å	Hetero 2-mer	54	-2.359
O14727	3JBT	Apoptotic protease-activating factor 1	3.80 Å	Hetero 14-mer	1248	
Q14790	1QTN	Caspase-8	1.20 Å	Hetero 6-mer	479	-2.241
P55211	1NW9	Caspase-9	2.40 Å	Hetero 2-mer	416	-2.013
P42574	2J30	Caspase-3	1.40 Å	Hetero 8-mer	277	-1.354
P55212	3S70	Caspase-6	1.63 Å	Hetero 4-mer	293	-1.859
P55210	4JR2	Caspase-7	1.65 Å	Hetero 4-mer	303	-4.242

Figure 2 illustrates a molecular interaction diagram highlighting the binding mode of a ligand within a protein binding site. Key residues such as LEU59, SER62, LEU63, TRP107, VAL110, VAL111, PHE114, and LEU26 participate in the interaction. The ligand forms hydrogen bonds (e.g., with SER62, shown by pink arrows), indicating critical points of interaction stabilizing the ligand within the binding pocket. Hydrophobic interactions are predominant, involving residues like LEU and VAL, depicted by hydrophobic circles. A Pi-Pi stacking interaction with PHE114 (green arrow) and solvent exposure around the

ligand's oxygen group are also evident. The diagram provides a clear visualization of the spatial arrangement and types of interactions, crucial for understanding ligand affinity and specificity. Figure 3 illustrates the molecular binding interactions of a ligand within a protein binding site involving a diverse array of residues. The ligand forms hydrogen bonds (yellow dashed lines) with polar and charged residues such as ARG187 and GLU216, indicating critical stabilizing interactions. Hydrophobic residues like PHE219, VAL226, VAL292,



**Figure 3b:** Caspase-7(4JR2) - 2,4,6-Octatrienoic acid complex (2D)

and MET294 are involved in non-polar interactions, enhancing the ligand's affinity. A Pi-Pi stacking interaction with PHE221 (green arrow) is evident, contributing to aromatic stabilization. The diagram also showcases polar interactions with residues like THR183 and TYR223, emphasizing the ligand's multifaceted binding profile. Additionally, solvent exposure is noted near specific functional groups, reflecting the ligand's potential accessibility. This visualization is pivotal for understanding the ligand's binding specificity and optimizing its affinity for therapeutic or biochemical applications.

Table 2 presents the docking scores and structural characteristics of five key anti-apoptotic proteins involved in apoptosis regulation and ubiquitination pathways, emphasizing their interaction potential. The apoptosis regulator Bcl-2, resolved at 1.40 Å as a monomer with 239 residues, exhibits a docking score of -2.397, suggesting moderate binding affinity and reinforcing its role as an anti-apoptotic protein. Bcl-2-like protein 1, with the finest resolution of 1.30 Å, forms a homo 2-mer with 233 residues and demonstrates a docking score of -3.676,

indicating strong interaction potential crucial for apoptosis regulation. Similarly, Bcl-2-like protein 2, resolved at 2.00 Å as a homo 2-mer with 193 residues, displays a docking score of -2.917, reflecting good binding potential in apoptosis-related mechanisms. The induced myeloid leukemia cell differentiation protein Mcl-1, resolved at 1.56 Å as a monomer with 350 residues, exhibits the strongest docking score of -4.625, highlighting its significant binding potential and critical anti-apoptotic function, often associated with cancer cell survival. Lastly, the E3 ubiquitin-protein ligase XIAP, resolved at 2.00 Å as a hetero 2-mer with 497 residues, presents a docking score of -3.007, underscoring its potent inhibitory effects on apoptosis through caspase inhibition and ubiquitination regulation. These proteins, particularly Mcl-1 and Bcl-2-like protein 1, exhibit strong docking scores, indicating their crucial roles in apoptosis modulation and their potential as

**Table 2:** The docking scores and structural characteristics of five key anti-apoptotic proteins

Uniprot ID	PDB ID	Protein Name	Resolution (Å)	Global Stoichiometry	Residues	Docking Score
P10415	6GL8	Apoptosis regulator Bcl-2	1.40 Å	Monomer	239	-2.397
Q07817	7JGW	Bcl-2-like protein 1	1.30 Å	Homo 2-mer	233	-3.676
Q92843	2Y6W	Bcl-2-like protein 2	2.00 Å	Homo 2-mer	193	-2.917
Q07820	8T6F	Induced myeloid leukemia cell differentiation protein Mcl-1	1.56 Å	Monomer	350	-4.625
P98170	1G73	E3 ubiquitin-protein ligase XIAP	2.00 Å	Hetero 2-mer	497	-3.007

therapeutic targets in apoptosis-related diseases. Structural data further bolster their relevance in drug design initiatives. The nearest high score binding images are described in figures 4 to 7 (3D and 2D images). Figure 4 illustrates the molecular binding interactions of a ligand within a protein's active site. Key residues contributing to the interaction

include polar residues like SER106 and ASN136, charged residues such as ARG102 and ARG139, and hydrophobic residues like PHE97, PHE143, and LEU108. Hydrogen bonding is prominently depicted (yellow dashed lines), with the ligand forming a significant bond with LEU108 (pink arrow), stabilizing its position. Pi-Pi stacking

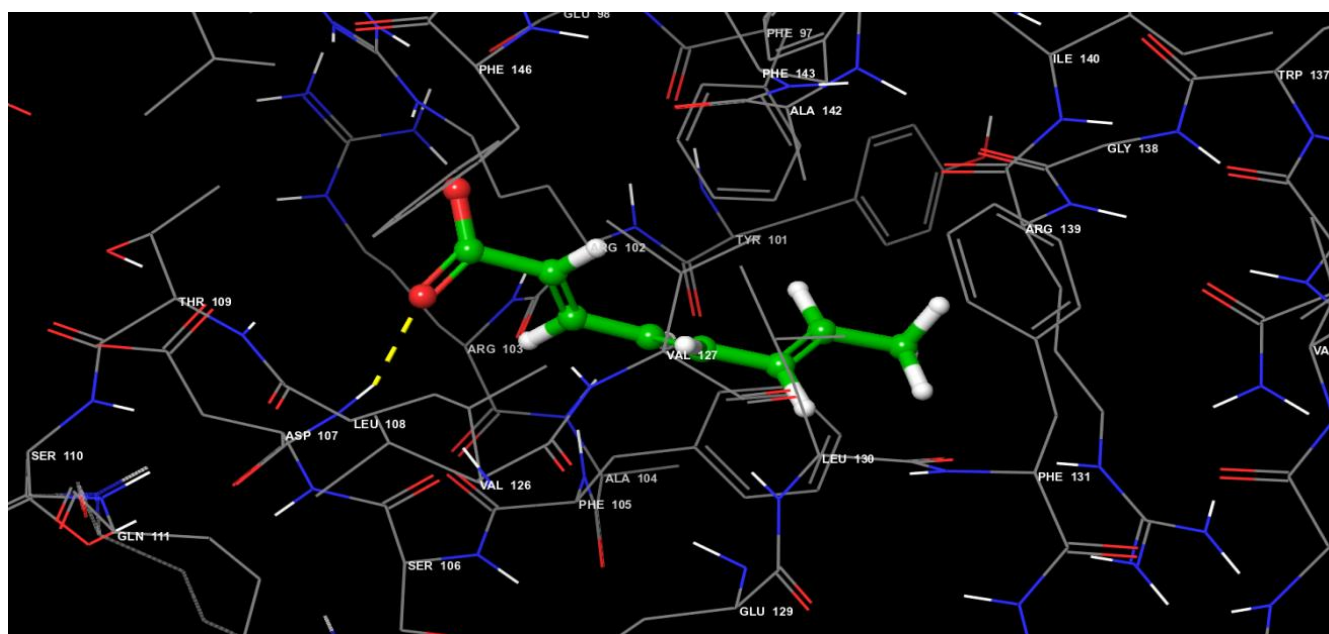
interactions (green arrow) are observed with PHE146, highlighting aromatic contributions to binding stability. Hydrophobic contacts with residues like ALA142 and PHE105 further enhance the ligand's affinity. The diagram also indicates solvent exposure and displaced hydration sites, reflecting the ligand's accessibility and its effect on the protein's microenvironment. This detailed visualization is critical for understanding ligand-protein interactions and optimizing ligand design for therapeutic purposes.

Figure 5 exhibits the molecular binding dynamics of a ligand within a protein's active site, highlighting key interactions with various residues. Notable hydrogen bonds are formed with LEU108 and other polar residues such as SER106 and ASN136, providing critical stabilization (depicted by yellow dashed and pink arrows). Pi-Pi stacking interactions with PHE146 enhance aromatic stabilization, while hydrophobic interactions involving residues like PHE143, PHE97, and ALA142 further contribute to the ligand's binding affinity. Charged residues, including ARG102 and ARG139, play a role in electrostatic interactions, while displaced hydration sites indicate the ligand's

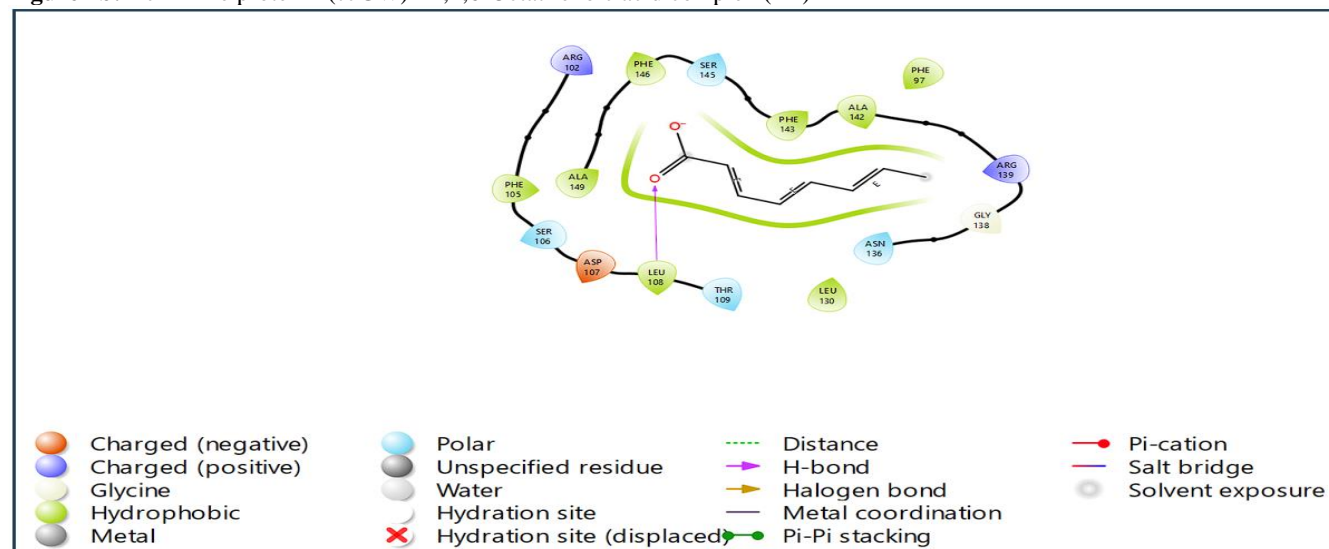
influence on the protein's water network. This comprehensive interaction network underscores the ligand's affinity and specificity within the binding pocket, offering valuable insights for drug design and molecular optimization.

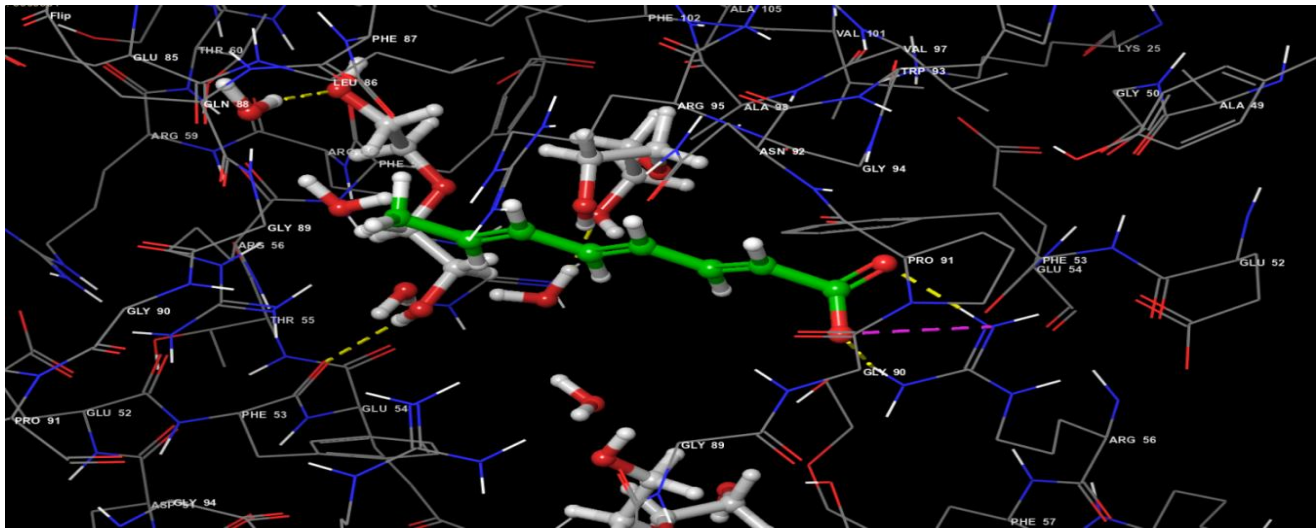
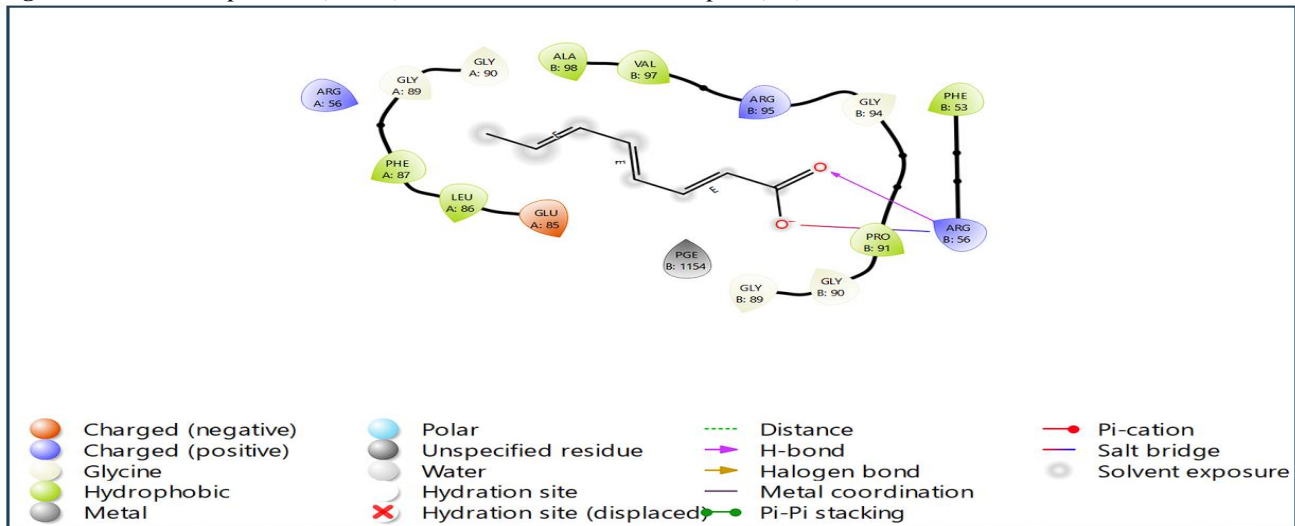
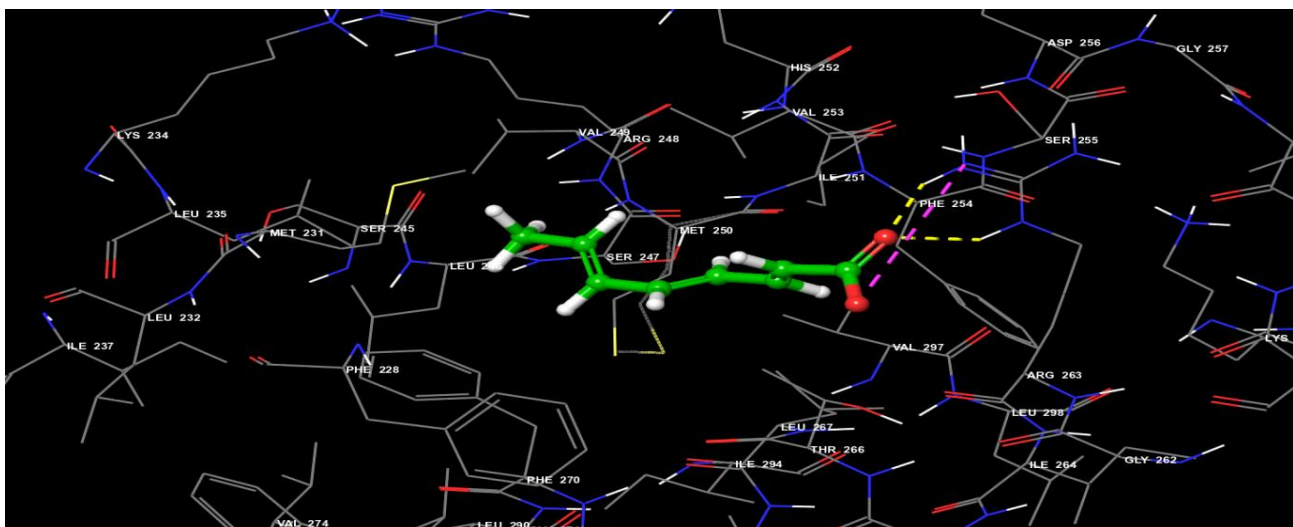
The molecular binding interactions between a ligand and its surrounding amino acid residues within a protein binding site are shown in figure 6. The key interactions include hydrophobic contacts with residues such as LEU 231, LEU 235, MET 250, VAL 249, VAL 253, PHE 254, and LEU 267, as indicated by green highlights. A polar interaction is observed with ARG 263, and a hydrogen bond is formed with THR 266, signifying the ligand's strong affinity for the binding site. The structural visualization also shows a displaced hydration site and solvent exposure, emphasizing the dynamic nature of the binding environment. This depiction aids in understanding the molecular docking and interaction mechanisms within the protein-ligand complex. The molecular interaction analysis between 2,4,6-Octatrienoic acid and various apoptosis-regulating proteins provides valuable insights into the

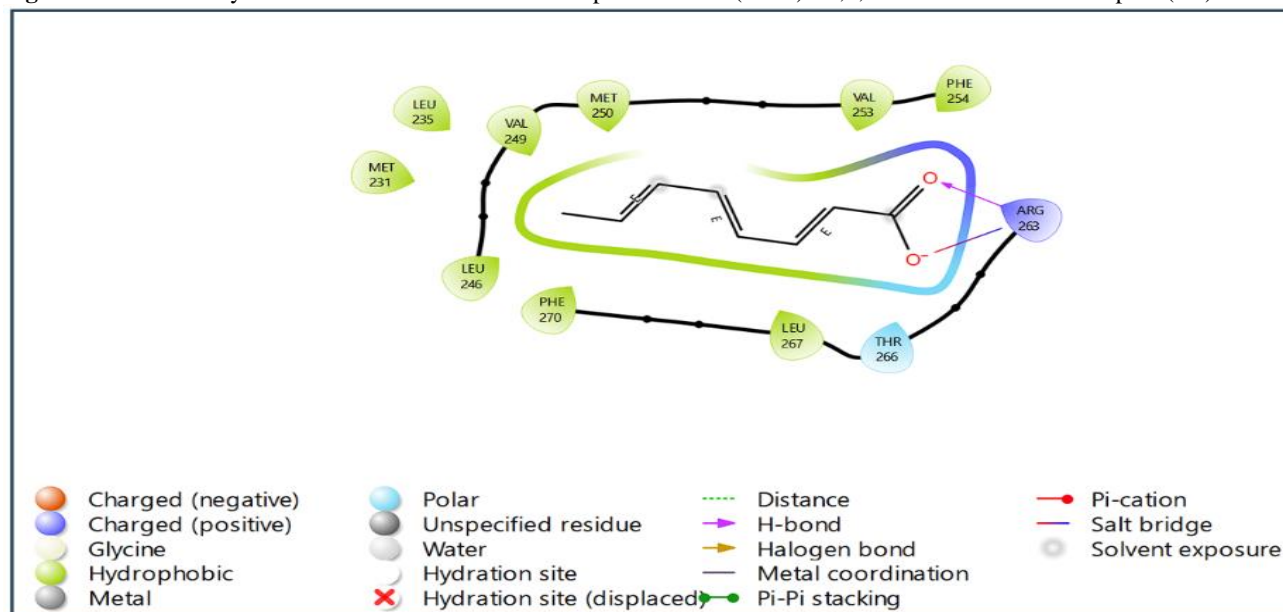
**Figure 4a:** Bcl-2-like protein 1(7JGW) - 2,4,6-Octatrienoic acid complex (3D)



**Figure 4b:** Bcl-2-like protein 1(7JGW) - 2,4,6-Octatrienoic acid complex (2D)



**Figure 5a:** Bcl-2-like protein 2(2Y6W) - 2,4,6-Octatrienoic acid complex (3D)**Figure 5b:** Bcl-2-like protein 2(2Y6W) - 2,4,6-Octatrienoic acid complex (2D)**Figure 6a:** Induced myeloid leukemia cell differentiation protein Mcl-1(8T6F) - 2,4,6-Octatrienoic acid complex (3D)

**Figure 6b:** Induced myeloid leukemia cell differentiation protein Mcl-1(8T6F) - 2,4,6-Octatrienoic acid complex (2D)

compound's potential biochemical effects is illustrated as figure 7. These complexes, including proteins such as Diablo IAP-binding mitochondrial protein (1G73), E3 ubiquitin-protein ligase XIAP (1NW9), caspases-7 and -8, as well as regulators like BAX, Bcl-2, and Mcl-1, suggest significant binding affinity that could influence apoptotic pathways. The structural integration of 2,4,6-Octatrienoic acid with these targets highlights its potential role in modulating cell death mechanisms, which might be useful for therapeutic applications in cancer or other apoptosis-related disorders. The study emphasizes the importance of ligand-protein interactions in drug discovery and their implications in targeted treatments. Table 3 examines the docking scores and structural characteristics of three key regulatory proteins involved in apoptosis and cellular stress response, highlighting their significance in therapeutic targeting. Cellular tumor antigen p53, resolved at 2.05 Å as a homo 4-mer with 393 residues, exhibits a docking score of -1.296. As a central regulator of DNA damage repair and apoptosis induction, its moderate docking score suggests specific binding limitations. Cytochrome c, with a high resolution of 1.36 Å, forms a homo 2-mer with 105 residues and has a docking score of -1.649. This protein plays a crucial role in the intrinsic apoptotic pathway by facilitating caspase activation upon mitochondrial release. Apoptosis-inducing factor 1, resolved at 1.75 Å as a monomer with 613 residues, displays a strong docking score of -3.593, emphasizing its role in mediating caspase-independent apoptosis while maintaining mitochondrial integrity under cellular stress.

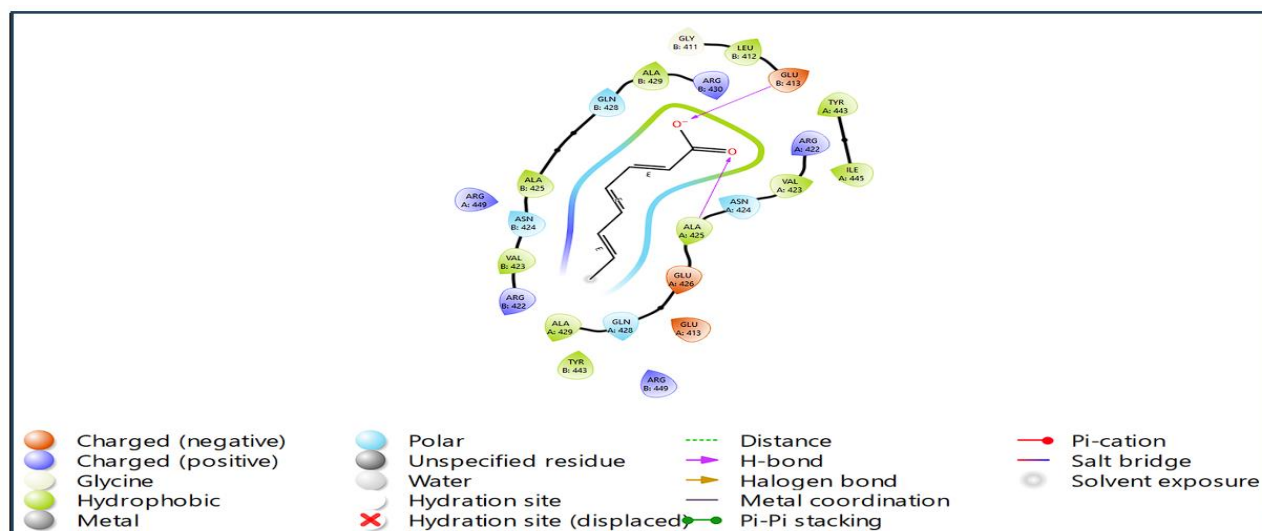
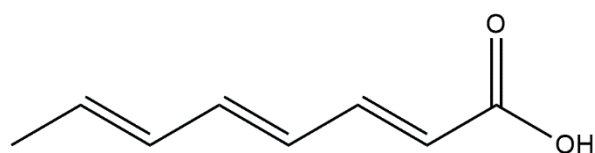
Among these proteins, apoptosis-inducing factor 1 displays the most favorable docking score, highlighting its significant binding potential. Cytochrome c and p53 also hold critical roles in apoptotic pathways, with structural and docking data providing a foundation for therapeutic applications targeting apoptosis-related disorders. The nearest high score binding images are described in figure 8 (3D and 2D images).

Figure 8 illustrates the binding site interactions of a ligand within a protein environment. The ligand forms significant interactions with various amino acid residues. Hydrophobic interactions are observed with residues such as LEU 8-412, VAL 8-424, TYR 8-443, and ILE 8-445, enhancing the ligand's stability within the binding pocket. Polar interactions include hydrogen bonding with residues GLN 8-425 and ASN 8-424, which contribute to the ligand's specificity. ARG 8-449 engages in a salt bridge, indicating strong ionic interaction. Additionally, residues such as GLU 8-413 and GLU 8-426 provide charged interactions, complementing the binding dynamics. The inclusion of a displaced hydration site and solvent exposure emphasizes the complex's adaptability in aqueous environments. This representation highlights the molecular basis of the ligand's binding affinity and selectivity. 2,4,6-Octatrienoic acid is a conjugated triene with three double bonds at positions 2, 4, and 6 in a trans, trans, trans configuration (figure 9). It has an eight-carbon backbone with a terminal carboxyl (-COOH) group, contributing to its stability and potential biological activity.

**Table 3:** The docking scores and structural features of four critical apoptotic regulatory proteins

Uniprot ID	PDB ID	Protein Name	Resolution (Å)	Global Stoichiometry	Residues	Docking Score
P04637	5O1I	Cellular tumor antigen p53	2.05 Å	Homo 4-mer	393	-1.296
P99999	5O1O	Cytochrome c	1.36 Å	Homo 2-mer	105	-1.649
O95831	5FS9	Apoptosis- inducing factor 1	1.75 Å	1.75 Å	613	-3.593



**Figure 8b:** Apoptosis-inducing factor 1(5FS9) - 2,4,6-Octatrienoic acid complex (2D)**Figure 9: Molecular Structure of 2,4,6-Octatrienoic acid**

2,4,6-Octatrienoic acid

#### Physicochemical Property

The molecule with the specified properties exhibits a molecular weight of 138.07, which falls within the optimal range of 100 to 600, making it suitable for biological systems. It has a Van der Waals volume of 153.959 Å<sup>3</sup> and a density of 0.897 g/cm<sup>3</sup>, calculated as the ratio of molecular weight to volume. The molecule features 2 hydrogen bond acceptors (nHA) and 1 hydrogen bond donor (nHD), both within the optimal ranges of 0–12 and 0–7, respectively, suggesting favorable interaction capabilities for potential biological activity. The molecule has 3 rotatable bonds (nRot), indicating moderate flexibility, with a flexibility ratio of 0.75 derived from the number of rotatable bonds divided by the number of rigid bonds (nRig = 4). It contains no rings (nRing = 0) or stereocenters, simplifying its structural complexity. The topological polar surface area (TPSA) is 37.3 Å<sup>2</sup>, within the ideal range for bioavailability (0–140 Å<sup>2</sup>), while its lipophilicity values, logP = 1.574 and logD = 1.539, indicate a balanced hydrophilic-lipophilic profile for drug-like properties. The molecule exhibits an acidic pKa of 4.235 and a basic pKa of 4.003, reflecting its ionization behavior in physiological conditions. Its melting point is 176.352°C, classifying it as a solid, and the boiling point of 246.872°C signifies thermal stability. With a predicted logS of -1.972, the molecule shows moderate solubility, crucial for bioavailability. These properties collectively suggest that the molecule is well-suited for drug discovery and development applications.

#### Medicinal Chemistry

The molecule exhibits a QED score of 0.476, categorizing it as moderately unattractive for drug-likeness since it falls in the 0.49–0.67 range. The GASA score of 0.0 indicates that the molecule is easy to synthesize. Similarly, a synthetic accessibility (Synth) score of 2.0 suggests that the molecule is relatively simple to synthesize, as scores below 6 are considered favorable. However, the Fsp<sup>3</sup> value of 0.125 indicates a low fraction of sp<sup>3</sup> carbons, potentially impacting solubility

and biological activity, as values above 0.42 are typically preferred. The MCE-18 score of 0.0 reflects poor medicinal chemistry evolution, which could limit its appeal for development. The natural product-likeness score (NPscore) of 1.604 signifies a moderate resemblance to natural products, enhancing its desirability as a lead compound. It adheres to the Lipinski, Pfizer, and GSK rules, which suggests favorable drug-likeness and ADMET profiles. Additionally, its Golden Triangle score of 1.0 places it within an optimal range (200 ≤ MW ≤ 500 and -2 ≤ logD ≤ 5), further supporting its drug development potential. The molecule raises no PAINS or ALARM NMR alerts, indicating the absence of frequent hitters or thiol-reactive properties. However, the BMS alert of 1 flags it as potentially undesirable or reactive, which may warrant further evaluation. With a colloidal aggregator score of 0.009, the molecule is unlikely to aggregate in a colloidal form, which is favorable. For ADMET profiles, it has a moderate probability (0.665) of being an fLuc inhibitor, indicating possible interference in luciferase-based assays. The probabilities for blue fluorescence (0.012) and green fluorescence (0.018) are low, suggesting minimal interference in fluorescence assays. However, the molecule is flagged as a reactive compound (score: 1.0) and shows a high probability (0.78) of being a promiscuous compound, which may contribute to nonspecific biological interactions. These properties highlight its potential while indicating areas for optimization.

#### Absorption

The molecule's absorption and permeability properties reveal a mixed profile. Its Caco-2 permeability score of -4.743 log unit is above the optimal threshold (-5.15), indicating moderate permeability across intestinal cells. Similarly, the MDCK permeability value of -4.634 log unit suggests medium permeability, though it does not reach the high permeability classification (> 20 × 10<sup>-6</sup> cm/s). The PAMPA permeability value of 0.992 logPeff falls below the threshold for high permeability (>2.5), indicating low passive permeability.

The molecule is a probable non-inhibitor of P-glycoprotein (Pgp), as shown by its low Pgp-inhibitor probability of 0.001, reducing the risk of drug efflux-related interactions. However, it has a moderate likelihood (0.35) of being a Pgp substrate, indicating possible transport by this efflux pump. The human intestinal absorption (HIA) probability of 0.234 places it in the HIA- category, signifying less than 30% absorption, which could limit its oral bioavailability.

Regarding bioavailability, the molecule shows probabilities of 0.682, 0.642, and 0.805 for F20%, F30%, and F50%, respectively. These scores suggest that the molecule is more likely to exhibit bioavailability below 50%, particularly falling below the 20% and 30% thresholds, which could impact its systemic exposure after oral administration. These findings highlight the molecule's potential absorption challenges

and its dependence on further structural optimization for improved bioavailability and permeability.

#### *Distribution*

The molecule demonstrates a plasma protein binding (PPB) value of 44.346%, which is within the optimal range (<90%), suggesting that a significant proportion of the drug remains free and pharmacologically active, potentially enhancing its therapeutic efficacy. Its volume of distribution (VD<sub>ss</sub>) value of -0.656 L/kg falls outside the optimal range (0.04–20 L/kg), indicating limited tissue distribution, which may restrict its therapeutic potential to plasma and extracellular spaces. The molecule is classified as BBB- with a 0.0 probability of blood-brain barrier (BBB) penetration, implying minimal likelihood of central nervous system (CNS) activity. Its fraction unbound in plasma (F<sub>u</sub>) is 48.519%, considered high (>20%), suggesting a significant amount of the drug remains unbound and readily available for distribution and metabolism. In terms of transporter interactions, the molecule shows a high probability (0.919) of being an OATP1B1 inhibitor and a moderate probability (0.521) of being an OATP1B3 inhibitor, indicating potential interactions with these hepatic transporters, which could influence drug disposition. Conversely, it has a low probability of inhibiting other transporters, including BCRP (0.006) and MRP1 (0.276), minimizing the risk of efflux-related drug-drug interactions.

These findings suggest that while the molecule exhibits favorable plasma protein binding and bioavailability characteristics, its limited tissue distribution and transporter inhibition profile warrant further investigation to optimize its pharmacokinetic properties.

#### *Metabolism*

The molecule exhibits a low probability of inhibition or substrate activity for most cytochrome P450 (CYP) isoforms, indicating a minimal risk of drug-drug interactions via these metabolic pathways. Specifically, it has a 0.031 probability of being a CYP1A2 inhibitor and a 0.001 probability of being a CYP1A2 substrate, highlighting its negligible impact on this isoform. Similarly, it shows very low probabilities of interaction with CYP2C19 (0.003 as an inhibitor, 0.007 as a substrate) and CYP3A4 (0.003 as an inhibitor, 0.0 as a substrate). For CYP2C9, the molecule has a slightly higher substrate probability (0.22) but remains a weak inhibitor (0.038). Its activity towards CYP2D6 is minimal, with 0.013 as an inhibitor and 0.001 as a substrate. Furthermore, the molecule does not act as a substrate for CYP2B6 (0.0) or CYP3A4 (0.0), and it exhibits low inhibition potential for CYP2B6 (0.037). However, it shows a high probability (0.982) of being a CYP2C8 inhibitor, which may have implications for drugs metabolized by this isoform. The molecule demonstrates poor human liver microsomal (HLM) stability, with a 0.175 probability of instability, suggesting it may undergo rapid metabolism in the liver. These results imply that the molecule has a favorable metabolic profile for most CYP pathways but requires careful evaluation of potential interactions involving CYP2C8 and its overall hepatic stability.

#### *Excretion*

The molecule exhibits a predicted plasma clearance (CL<sub>plasma</sub>) of 3.153 ml/min/kg, categorizing it as having low clearance. This suggests that the compound is eliminated at a slower rate from the bloodstream, potentially leading to prolonged systemic exposure. The predicted half-life (T<sub>1/2</sub>) of the compound is 1.694 hours, classifying it as a short half-life drug. Drugs with such a profile typically require frequent dosing to maintain therapeutic levels. Overall, the compound's clearance and half-life indicate that it has moderate pharmacokinetic properties, but its short half-life might limit its duration of action, necessitating appropriate formulation adjustments or dosing strategies.

#### *Toxicity*

The compound exhibits a low probability of hERG inhibition, with values of 0.037 and 0.069 for different thresholds, indicating a reduced risk of cardiac toxicity. However, the Drug-Induced Liver Injury (DILI) score of 0.822 suggests a high risk of hepatotoxicity, warranting careful monitoring in further evaluations. Similarly, the Ames Mutagenicity score of 0.492 implies a moderate likelihood of mutagenic potential.

For acute toxicity, the Rat Oral Acute Toxicity score of 0.272 places the compound in the low-toxicity category (>500 mg/kg). The FDA Maximum Daily Dose (FDAMDD) score of 0.335 also suggests moderate safety regarding dose limitations. Notably, the compound shows high probabilities for skin sensitization (0.681), eye irritation (0.989), and respiratory toxicity (0.79), indicating potential adverse effects on skin, eyes, and respiratory health. Furthermore, it has a moderate probability of hepatotoxicity (0.643) and nephrotoxicity (0.593), suggesting possible risks to liver and kidney function. The cytotoxicity scores for RPMI-8226, A549, and HEK293 cells are low (0.031, 0.01, and 0.049, respectively), indicating minimal cytotoxic effects. However, the genotoxicity score (0.574) suggests moderate potential for genetic damage, while the neurotoxicity score (0.247) implies a low risk of neurotoxicity. Overall, the compound shows mixed toxicological properties, requiring further optimization and testing.

#### *Environmental Toxicity*

The key ecotoxicological properties and their corresponding values, essential for environmental risk assessments, provide insight into potential ecological hazards. The Bioconcentration Factor (0.304) evaluates the likelihood of secondary poisoning and human health risks through the food chain, expressed in a logarithmic unit incorporating molecular weight. The IGC<sub>50</sub> value (2.885) represents the concentration required to inhibit 50% growth in *Tetrahymena pyriformis*, a protozoan, offering a crucial measure of aquatic toxicity. Similarly, the LC<sub>50</sub>FM value (3.3) denotes the 96-hour lethal concentration causing 50% mortality in fathead minnows, serving as a critical indicator of fish toxicity. Additionally, the LC<sub>50</sub>DM value (3.896) reflects the 48-hour lethal concentration for 50% mortality in *Daphnia magna*, a freshwater crustacean, highlighting its susceptibility to toxic exposure. These parameters collectively aid in evaluating environmental hazards and informing regulatory decisions. These metrics highlight the sensitivity of aquatic organisms to chemical exposure and are critical for understanding environmental impacts.

#### *Toxicity Pathway*

The activity probabilities of various nuclear receptors (NR) and stress response (SR) pathways provide critical insights into molecular interactions and toxicity mechanisms. Among nuclear receptors, the Aryl hydrocarbon receptor (NR-AhR), Androgen receptor (NR-AR) and its ligand-binding domain (NR-AR-LBD), Aromatase (NR-Aromatase), and Peroxisome proliferator-activated receptor gamma (NR-PPAR-gamma) are all classified as inactive, each with a probability of 0.0. The Estrogen receptor (NR-ER) exhibits a minimal activity probability of 0.012, while its ligand-binding domain (NR-ER-LBD) remains inactive. In the stress response pathways, the Antioxidant Response Element (SR-ARE) shows high activity with a probability of 0.934, suggesting a strong interaction, whereas ATPase family AAA domain-containing protein 5 (SR-ATAD5) remains inactive. The Heat Shock Factor Response Element (SR-HSE) and the Mitochondrial Membrane Potential pathway (SR-MMP) display minimal activity probabilities of 0.021 and 0.005, respectively. Additionally, the tumor suppressor protein p53 (SR-p53) exhibits a low probability of activity at 0.033. This data serves as a valuable resource for risk assessments by identifying potential receptor and pathway interactions, aiding in toxicity prediction and molecular mechanism evaluation.

#### *Toxicophore Rules*

An evaluation of various toxicity and chemical property rules, based on structural alerts and substructures, provides critical insights into potential risks and environmental or biological impacts. The Acute Toxicity Rule detects no alerts among 20 substructures, indicating no immediate concerns for acute oral toxicity. Similarly, the Genotoxic Carcinogenicity Rule identifies no alerts within 117 substructures associated with carcinogenicity or mutagenicity. However, the Non-Genotoxic Carcinogenicity Rule highlights one alert among 23 substructures, suggesting potential carcinogenicity through non-genotoxic mechanisms. The Skin Sensitization Rule detects two alerts within 155 substructures, pointing to possible skin irritation risks. Likewise, the Aquatic Toxicity Rule identifies two alerts among 99

substructures, indicating potential toxicity in aquatic environments. In contrast, the Non-Biodegradable Rule finds no alerts within 19 substructures, suggesting no biodegradability concerns. The SureChEMBL Rule and FAF-Drugs4 Rule both detect two alerts, with SureChEMBL flagging potential medicinal chemistry-unfriendly characteristics among 164 substructures, while FAF-Drugs4 identifies toxicity risks within 154 substructures cataloged in its database. These findings provide valuable insights into potential risks and environmental or biological impacts based on structural properties.

## Conclusion

The findings of this study underscore the strong binding affinity of 2,4,6-Octatrienoic acid with key apoptotic markers, including Caspase-7, BAX, Bcl-2-like proteins 1 and 2, Mcl-1, XIAP, and Apoptosis-inducing factor 1, primarily mediated through significant interactions such as hydrogen bonding. These results highlight the potential of 2,4,6-Octatrienoic acid as a promising modulator of apoptotic pathways, paving the way for its potential application in the therapeutic development of diseases associated with dysregulated apoptosis such as cancer. However, further research, including experimental validation and comprehensive pharmacological assessments, is essential to confirm its therapeutic efficacy and explore its broader applications.

## Conflict of interest

The author reports no conflicts of interest in this work.

## Authors' Declaration

The authors hereby declare that the work presented in this article is original and that any liability for claims relating to the content of this article will be borne by them.

## References

- Mustafa M, Ahmad R, Tantry IQ, Ahmad W, Siddiqui S, Alam M, Abbas K, Moinuddin, Hassan MI, Habib S, Islam S. Apoptosis: A comprehensive overview of signaling pathways, morphological changes, and physiological significance and therapeutic implications. *Cells*. 2024; 13(22):1-29
- Engel N, Falodun A, Kühn J, Kragl U, Langer P, Nebe B. Pro-apoptotic and anti-adhesive effects of four African plant extracts on the breast cancer cell line MCF-7. *BMC Complement Altern Med*. 2014; 14(33):334-347
- Karthik M, Paari E, Sivasankaran SM, Elanchezhian C, Manoharan S. Ursolic acid-loaded chitosan nanoparticles modulate the expression pattern of apoptotic markers towards oral tumour inhibition in golden Syrian hamsters. *Trop J Nat Prod Res*. 2023; 7(11):5250-5255.
- Kristianingsih A, Reviono R, Wasita B. Molecular docking study of quercetin from ethanol extract of *Mimosa pudica* Linn on asthma biomarkers. *Trop J Nat Prod Res*. 2024; 8(10):8640-8645.
- National Center for Biotechnology Information. PubChem compound summary for CID 5368831, 2,4,6-Octatrienoic acid. 2025. Available from: <https://pubchem.ncbi.nlm.nih.gov/compound/Octa-2,4,6-trienoic-acid>. Accessed Feb. 15, 2025.
- Flori E, Mastrofrancesco A, Kovacs D, Ramot Y, Briganti S, Bellei B, Paus R, Picardo M. 2,4,6-Octatrienoic acid is a novel promoter of melanogenesis and antioxidant defence in normal human melanocytes via PPAR- $\gamma$  activation. *Pigment Cell Melanoma Res*. 2011; 24(4):618-630.
- Flori E, Mastrofrancesco A, Kovacs D, Bellei B, Briganti S, Maresca V, Cardinali G, Picardo M. The activation of PPAR $\gamma$  by 2,4,6-Octatrienoic acid protects human keratinocytes from UVR-induced damages. *Sci Rep*. 2017; 7(1):9241.
- Pinzi L, Rastelli G. Molecular docking: Shifting paradigms in drug discovery. *Int J Mol Sci*. 2019; 20(18) 1-23
- Spassov DS. Binding affinity determination in drug design: insights from lock and key, induced fit, conformational selection, and inhibitor trapping models. *Int J Mol Sci*. 2024; 25(13):1-13.
- Berman HM, Westbrook J, Feng Z, Gilliland G, Bhat TN, Weissig H, Shindyalov IN, Bourne PE. The protein data bank. *Nucleic Acids Res*. 2000; 28(1):235-242.
- Daina A, Michielin O, Zoete V. SwissADME: a free web tool to evaluate pharmacokinetics, drug-likeness and medicinal chemistry friendliness of small molecules. *Sci Rep*. 2017; 7:4271, 1-13
- Fu L, Shi S, Yi J, Wang N, He Y, Wu Z, Peng J, Deng Y, Wang W, Wu C, Lyu A, Zeng X, Zhao W, Hou T, Cao D. ADMETlab 3.0: An updated comprehensive online ADMET prediction platform enhanced with broader coverage, improved performance, API functionality and decision support. *Nucleic Acids Res*. 2024; 52(W1):W422-W431.
- He R, Liu Y, Fu W, He X, Liu S, Xiao D, Tao Y. Mechanisms and cross-talk of regulated cell death and their epigenetic modifications in tumor progression. *Mol Cancer*. 2024; 23(1):1-54
- Abaza A, Vasavada AM, Sadhu A, Valencia C, Fatima H, Nwankwo I, Anam M, Maharjan S, Amjad Z, Khan S. A systematic review of apoptosis in correlation with cancer: should apoptosis be the ultimate target for cancer treatment? *Cureus*. 2022; 14(8):e28496.
- Caro-Gómez LA, López-Hidalgo M, Rosas-Trigueros JL, Torres-Rivera A, Vázquez-Hernández JJ, Benítez-Cardoza CG. Identification of compounds against anti-apoptotic bcl-2 protein using docking studies. *ChemistrySelect*. 2024; 9(1):e202302948.
- Mohamad Rosdi MN, Mohd Arif S, Abu Bakar MH, Razali SA, Mohamed Zulkifli R, Ya'akob H. Molecular docking studies of bioactive compounds from *Annona muricata* Linn as potential inhibitors for Bcl-2, Bcl-w and Mcl-1 antiapoptotic proteins. *Apoptosis*. 2018; 23(1):27-40.
- Nurhayati APD, Rihandoko A, Fadlan A, Ghaissani SS, Jadid N, Setiawan E. Anti-cancer potency by induced apoptosis by molecular docking P53, caspase, cyclin D1, cytotoxicity analysis and phagocytosis activity of trisindoline 1,3 and 4. *Saudi Pharm J*. 2022; 30(9):1345-1359.
- Basumatary M, Talukdar A, Sharma M, Dutta A, Mukhopadhyay R, Doley R. Exploring the anticancer potential of Cytotoxin 10 from *Naja kaouthia* venom: Mechanistic insights from breast and lung cancer cell lines. *Chem Biol Interact*. 2024; 403:111254-111257